Dyes and Pigments 89 (2011) 23–28

Contents lists available at ScienceDirect

Dyes and Pigments

journal homepage: www.elsevier.com/locate/dyepig

Synthesis and properties of novel perylenetetracarboxylic diimide derivatives fused with BODIPY units

Junqian Feng [a,b], Delou Wang [a], Shuangqing Wang [c], Liangliang Zhang [a], Xiyou Li [a,*]

[a] Key Lab for Colloid and Interface Chemistry of Education Ministry, Department of Chemistry, Shandong University, Jinan 250100, China
[b] College of Shandong Policeman, Jinan 250014, China
[c] Key Laboratory of Photochemistry of CAS, Institute of Chemistry, Chinese Academy of Science, Beijng 100800, China

ARTICLE INFO

Article history:
Received 30 June 2010
Received in revised form
20 August 2010
Accepted 24 August 2010
Available online 21 September 2010

Keywords:
Perylenetetracarboxylic diimide
Methylquinoline
Methylpyridine
BODIPY
Synthesis
Photophysical properties

ABSTRACT

Two novel fluorescent dyes based on perylenetetracarboxylic diimde (PDI) with methylpyridine or methylquinoline group at the carbonyl position were designed and synthesized. Their structures were confirmed by ^{1}H NMR, ^{13}C NMR, MS, and elementary analysis. The resulted new compounds show longer wavelength absorption with relative high extinction coefficient and red-shifted emission with high fluorescence quantum yields. These compounds can further react with $BF_3 \cdot Et_2O$ to form novel dyes containing BODIPY (difluoroboradiazaindacene) analogue unit, by which both the absorption and emission maximum have been red-shifted further. The minimized structures based on density function theory (DFT) calculation show planar configurations for the compounds. The calculated molecular orbital correlates well with their red-shifted absorption and emission spectra.

1. Introduction

Perylenetetracarboxylic diimides (PDIs) have found wide rang applications in diverse fields of current research because of their excellent thermal and photo-stability, high luminescence efficiency, and novel optoelectronic properties [1–4]. Driven by the demands of varies applications, the modification on molecular structure of PDIs with intention to tune the photophysical properties has attracted a lot of research interest in the past decade [5–12]. The modifications on molecular structure of PDI are usually achieved by introducing side groups to the imide nitrogen atoms or at the bay positions. Incorporation of substituents onto the imide nitrogen atoms could improve the solubility of PDIs in solvents and affect the packing behavior of PDIs in the solid state [13–22], but did not change the photophysical properties significantly. However, the introduction of substituents at the bay positions could change the photophysical properties of PDIs as well as improve the solubility of them in conventional organic solvents [7,23–27]. Recently, direct alkylation of PDIs at 2,5,8,11-positions has been achieved by the Murai–Chatani–Kakiuchi protocol. The resulted compounds show enhanced solubility and higher fluorescence quantum efficiency in solid state [28].

Fusing of aromatic rings with PDI conjugation system has turned into another efficient method to modify the molecular structure of PDI in the past several years, which could achieve significant property variation [29–33]. The famous “amidine” derivatives of PDI, developed by Langhals and Müllen groups [34–36], were prepared by the condensation of perylenetetracarboxylic dianhydride with diamino compounds. The absorption and fluorescence spectra of these compounds are red-shifted even up to the near infrared region. The cooperation of aromatic rings to the bay positions of PDI ring by Diels–Alder reactions has generated a series novel PDI compounds with longer wavelength absorption and emission [37]. A recent report on this topic described the cooperation of imidazole with PDI ring at the bay position by light driving cyclization [38]. The resulted compounds show red-shifted absorption and emission spectra as well as the structure tunable self-assembly. We have recently fused a difluoroboradiazaindacene (BODIPY) type ring with the PDI ring successfully by introducing 2-methylquinoline group at the imide nitrogen position of PDI [39]. The resulted new molecules show significantly red-shifted absorption and emission spectra with high fluorescence quantum yield.

In this paper, we present another way for the molecular structure modification of the PDI by introducing methylquinoline or

* Corresponding author. Tel.: +86 531 88564464; fax: +86 531 88369877.
E-mail address: xiyouli@sdu.edu.cn (X. Li).

0143-7208/$ – see front matter © 2010 Elsevier Ltd. All rights reserved.
doi:10.1016/j.dyepig.2010.08.014

methylpyridine groups at the carbonyl position (**1** and **2** in Fig. 1). To the best of our knowledge, this is the first example that substituent has been selectively introduced to the carbonyl group of PDI. The resulted new compounds show significantly red-shifted absorption and emission spectra with large extinction co-efficiency and reasonable fluorescence quantum yield. More interestingly, these novel compounds can further react with $BF_3 \cdot Et_2O$ to introduce BODIPY type structure characteristics into the PDI molecules (**3** and **4** in Fig. 1).

2. Experimental

2.1. General methods

^1H and ^{13}C NMR spectra were recorded on a Bruker 300 MHz NMR spectrometer with chemical shifts reported in ppm (in $CDCl_3$, TMS as internal standard). MALDI-TOF mass spectra were taken on a Bruker/ultra flex instrument. Absorption spectra were measured on HITACHI U-4100 spectrophotometer. Fluorescence spectra and fluorescence lifetime were measured on an ISS K2 system. The fluorescence lifetimes were measured with a phase modulation model with a scattering sample as standard. The fluorescence quantum yields were determined according to Equation (1).

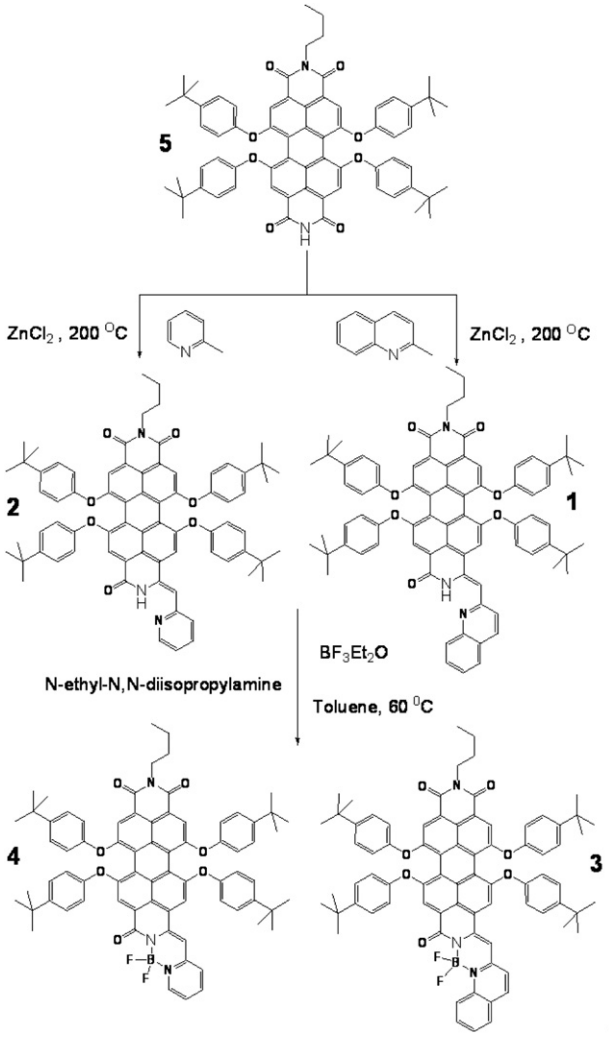

Fig. 1. Synthesis of compound **1**–**4**.

$$\frac{\Phi_S}{\Phi_R} = \frac{M_S A_R n_S^2}{M_R A_S n_R^2} \quad (1)$$

where Φ represents Fluorescence quantum yield, and M, the emission intensity, was calculated from the spectrum area, A represents the optical density at the excitation wavelength and n the refraction coefficient of each solvent. The superscripts "S" and "R" refer to the sample and to the standard, respectively. Fluorescence quantum yield was determined on the basis of the absorption and fluorescence spectra. N,N′-dicyclohexylperylene-3,4:9,10-tetra carboxylic diimide was used as a reference ($\Phi = 100\%$ in CH_2Cl_2).

2.2. Computation details

The hybrid density function B3LYP (Becke–Lee–Young–Parr composite of exchange-correction functional) method [40,41] and the standard 6–31G(d) basis set [42] were used for both structure optimization and the property calculations. All the calculations were performed using the Gaussian 03 program in the IBM P690 system at the Shandong Province High Performance Computing Centre.

2.3. Materials

N,N′-dibutyl-1,6,7,12-tetra(4-*tert*-butylphenoxy)perylene-3,4:9,10-tetra carboxylic diimide (**6**) [43] were prepared following the literature method and fully characterized by ^1H NMR and MALDI-TOF mass spectra. All other chemicals are purchased from commercial source. Solvents were of analytical grades and were purified by the standard method before use.

2.3.1. *N-n-Butyl-1,6,7,12-tetra(4-tert-butylphenoxy)-3,4:9,10-perylenetetra-carboxdiimide (**5**)*

A solution of N-n-Butyl-1,6,7,12-tetra(4-*tert*-butylphenoxy)perylene-3,4-anhydride-9,10-imide [39] (1.0 g, 1.15 mmol) in methanamide (100 ml) was purged with nitrogen for 15 min and then was heated to reflux. The resulting mixture was kept at reflux continuously for another 16 h, and then was poured into water. The solid was collected by filtration and purified by column chromatography on silica gel with chloroform as the eluent. Repeated chromatography followed by recrystallization from a mixture of $CHCl_3$ and MeOH gave pure product **5** (0.62 g, yield 52%): mp. > 300 °C; ^1H NMR (300 MHz, $CDCl_3$) δ 8.38 (s, 4H), 8.22 (s, 4H), 7.24 (m, 8H), 6.82 (m, 8H), 4.11 (t, 2H), 1.65 (m, 2H), 1.40(m, 2H), 1.29 (s, 36H), 0.93 (t, 3H); MALDI-TOF MS (*m/z*) 1039.2, Calcd for $C_{68}H_{66}N_2O_8$ (*m/z*) 1039.3. Anal. Calcd. for $C_{68}H_{66}N_2O_8$: C, 78.59; H, 6.40; N, 2.70. Found: C, 78.52; H, 6.38; N, 2.79.

*2.4.1. Compound **1**.* A mixture of **5** (0.20 g, 0.19 mmol), 2-methylquinoline (2 g, 14 mmol) and fresh dried zinc chloride (2 g, 15 mmol) was heated to 200 °C for 15 min. The reaction mixture was extracted several times with dichloromethane. The combined extract was dried over sodium sulfate for overnight and then was evaporated to dry. The red solid collected was purified by column chromatography on silica gel with dichloromethane as eluent. Compound **1** was afforded as green powder (0.10 g, 46%): mp. > 300 °C; UV–vis (CH_2Cl_2, ε) 626 nm (6.25×10^4 L mol^{-1} cm^{-1}); ^1H NMR (300 MHz, $CDCl_3$) δ 14.37 (s, 1H), 8.20 (s, 1H), 8.16 (s, 1H), 8.15 (s, 1H), 8.12 (d, 1H), 8.00 (d, 1H), 7.84 (s, 1H), 7.69 (t, 2H), 7.44 (m, 1H), 7.41 (m,1H), 7.27 (m, 8H), 6.84 (m, 8H), 6.36 (s, 1H), 4.10 (t, 2H), 1.66 (m, 2H), 1.42 (m, 2H), 1.31 (s, 36H), 0.94 (t, 3H); ^{13}C NMR (100 Hz, $CDCl_3$) δ 163.0, 160.5, 155.7, 155.5, 154.8, 153.4, 152.6, 146.5, 146.3, 146.1, 139.1, 135.8, 133.3, 132.9, 129.6, 127.9, 126.8, 126.1, 125.7, 125.6, 124.6, 122.9, 121.1, 121.0, 120.8, 120.4, 119.1, 118.8, 118.7, 118.1, 117.5, 116.7, 112.1, 100.9, 39.8, 33.8, 31.0, 29.7, 29.2, 19.7, 13.3; MALDI-TOF MS (*m/z*) 1164.3, Calcd.

For $C_{78}H_{73}N_3O_7$ (*m/z*) 1164.4. Anal. Calcd. For $C_{78}H_{73}N_3O_7$: C, 80.45%; H, 6.32%; N, 3.61%. Found: C, 80.39%; H, 6.35%; N, 3.63%.

2.4.2. Compound ***2***. A mixture of **5** (0.20 g, 0.19 mmol), 2-methylpyridine (2 g, 21 mmol) and fresh dried zinc chloride (2 g, 15 mmol) was heated to 200 °C for 30 min. The reaction cake was extracted several times with dichloromethane. The combined extract was dried over sodium sulfate for overnight and then was evaporated to dry. The red solid collected was purified by column chromatography on silica gel with dichloromethane as eluent. Compound **2** was afforded as green powder (0.09 g, 42%): mp. > 300 °C; UV–vis (CH_2Cl_2, ε) 615 nm (5.35×10^4 L mol^{-1} cm^{-1}); ^{1}H NMR (300 MHz, $CDCl_3$) δ 13.67 (s, 1H), 8.63 (d, 1H), 8.21 (s, 1H), 8.17 (s, 1H), 8.13 (s, 1H), 7.80 (s, 1H), 7.62 (m, 2H), 7.28 (s, 1H), 7.25 (m, 8H), 6.83 (m, 8H), 6.26 (s, 1H), 4.11 (t, 2H), 1.64 (m, 2H), 1.43 (m, 2H), 1.38 (s, 36H), 0.93 (t, 3H); ^{13}C NMR (100 Hz, $CDCl_3$) δ 163.1, 160.4, 155.8, 155.6, 154.8, 154.7, 154.3, 153.4, 152.7, 147.7, 146.5, 146.4, 146.1, 137.4, 136.1, 133.3, 133.0, 126.2, 126.1, 126.0, 124.7, 124.2, 121.0, 120.9, 120.7, 120.4, 120.0, 119.5, 119.1, 118.9, 118.8, 118.7, 118.1, 117.1, 116.6, 111.9, 101.3, 39.8, 33.8, 31.0, 29.7, 29.2, 19.9, 13.3; MALDI-TOF MS (*m/z*) 1114.3, Calcd. For $C_{74}H_{71}N_3O_7$ (*m/z*) 1114.4. Anal. Calcd. For $C_{74}H_{71}N_3O_7$: C, 79.76%; H, 6.42%; N, 3.77%. Found: C, 79.73%; H, 6.39%; N, 3.75%.

2.4.3. Compound ***3***. N-Ethyldiisopropylamine (0.5 ml) and $BF_3 \cdot Et_2O$ (1 ml) were added to the solution of compound **1** (0.1 g, 0.09 mmol) in toluene (15 ml). The mixture was heated at 60 °C and stirred under nitrogen for 2.5 h. The residue was purified by silica gel column chromatography with dichloromethane as eluent. Compound **3** was collected as green powder (0.06 g, yield 57%): mp. > 300 °C; UV–vis (CH_2Cl_2, ε) 648 nm (7.74×10^4 L mol^{-1} cm^{-1}); ^{1}H NMR (300 MHz, $CDCl_3$) δ 8.88 (d, 1H), 8.25 (s, 1H), 8.24 (s, 1H), 8.17 (s, 1H), 8.09 (d, 1H), 7.97 (s, 1H), 7.80 (t, 1H), 7.70 (m, 1H), 7.50 (m, 1H), 7.30 (s, 1H), 7.22 (m, 8H), 6.90 (m, 4H), 6.78 (m, 4H), 6.35 (s, 1H), 4.13 (t, 2H), 1.66 (m, 2H), 1.40 (m, 2H), 1.30 (s, 36H), 0.94 (t, 3H); ^{13}C NMR (100 Hz, $CDCl_3$) δ 163.5, 157.0, 155.6, 154.9, 154.0, 153.1, 152.6, 147.3, 147.2, 146.7, 141.0, 132.7, 130.9, 128.9, 126.8, 125.0, 123.4, 122.1, 121.9, 120.2, 119.8, 119.5, 119.2, 118.6, 118.4, 40.4, 34.7, 32.7, 31.5, 30.2, 21.4, 20.4, 13.8; MALDI-TOF MS (*m/z*) 1212.2, Calcd. For $C_{78}H_{72}BF_2N_3O_7$ (*m/z*) 1212.2. Anal. Calcd. For $C_{78}H_{72}BF_2N_3O_7$: C, 77.28%; H, 5.99%; N, 3.47%. Found: C, 77.33%; H, 5.83%; N, 3.45%.

2.4.4. Compound ***4***. N-Ethyldiisopropylamine (0.5 ml) and $BF_3 \cdot Et_2O$ (1 ml) were added to the solution of compound **2** (0.1 g, 0.09 mmol) in 15 ml toluene. The mixture was heated at 60 °C and stirred under nitrogen for 2.5 h. The residue was purified by silica gel column chromatography using dichloromethane as eluent. Compound **4** was collected as green powder (0.07 g, yield: 69%). mp. > 300 °C; UV–vis (CH_2Cl_2, ε) 624 nm (4.87×10^4 L mol^{-1} cm^{-1}); ^{1}H NMR (300 MHz, $CDCl_3$) δ 8.61 (d, 1H), 8.25 (s, 1H), 8.21 (s, 1H), 8.16 (s, 1H), 7.91 (s, 1H), 7.86 (m, 1H), 7.27 (s, 1H), 7.24 (m, 4H), 7.22 (m, 1H), 7.21 (m, 4H), 6.87 (m, 4H), 6.77 (m, 4H), 6.34 (s, 1H), 4.11 (t, 2H), 1.63 (m, 2H), 1.40 (m, 2H), 1.31 (s, 36H), 0.94 (t, 3H); ^{13}C NMR (100 Hz, $CDCl_3$) δ 163.6, 156.9, 155.4, 154.9, 154.1, 153.1, 147.3, 147.1, 146.6, 141.6, 133.3, 131.2, 126.6, 123.5, 122.0, 121.3, 120.1, 119.7, 119.6, 119.4, 119.2, 115.0, 40.4, 34.3, 31.0, 30.2, 29.7, 20.4, 13.8; MALDI-TOF MS (*m/z*) 1162.2, Calcd. For $C_{74}H_{70}BF_2N_3O_7$ (*m/z*) 1162.2. Anal. Calcd. For $C_{74}H_{70}BF_2N_3O_7$: C, 76.48%; H, 6.07%; N, 3.62%. Found: C, 76.53%; H, 6.04%; N, 3.59%.

3. Results and discussion

The synthetic procedures of compound **1**–**4** are shown in Fig. 1. Compound **1** and **2** were synthesized following a modified literature method [39,44,45]. Condensation of **5** with 2-methylquinoline or 2-methylpyridine was carried out without solvent using zinc chloride as catalyst. To obtain compound **1** or **2**, extra excess of zinc chloride and shorter reaction time compared with that of the literature method are necessary. Product **1** and **2** were collected from the reaction mixture with the yields of 46% and 42% respectively. Compound **1** or **2** reacts further with $BF_3 \cdot OEt_2$ in toluene at 60 °C in the presence of N-ethyl-N, N-di-*iso*-propylamine for 2.5 h to give **3** and **4** in yields of 57%, 69% respectively. All these compounds show good solubility in conventional halogenated organic solvents, but small solubility in alcoholic solvents. The structures of these compounds were fully characterized by different spectroscopic methods, including ^{1}H and ^{13}C NMR, MALDI-TOF mass spectrometry and elemental analysis. It is reasonable to expect the formation of *cis* and *trans* isomers of compound **1** and **2** due to the newly formed carbon–carbon double bond. However, the ^{1}H NMR spectra did not show any evidence to support the presence of isomers of compound **1** and **2**.

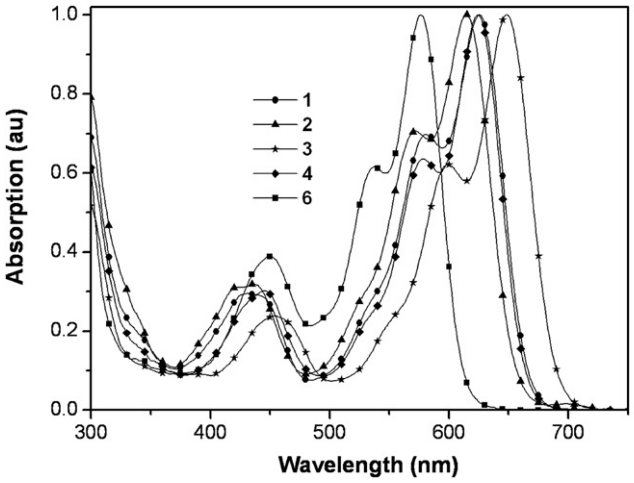

Fig. 2. Normalized absorption spectra of compound **1**–**4** compared with that of **6** in dichloromethane.

It is interesting that only the mono substituted compound **1** and **2** can be separated from the reaction mixture. Compounds with more methylpyridine or methylquinoline groups attached were not observed in the reaction mixture. This may be ascribed to the steric hindrance introduced by the butyl group at imide nitrogen and its electron donating nature, which reduce the reactivity of the carbonyl groups at this end of the PDI significantly. Meanwhile, the

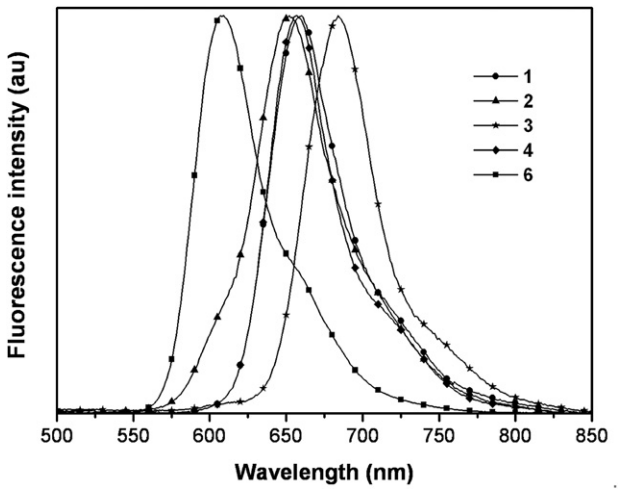

Fig. 3. Normalized fluorescence spectra of **1**–**4** compared with that of **6** in dichloromethane (excited at 450 nm).

Table 1
Photophysical properties of compound **1**–**4** and **6**.

Compounds	λ_{abs} (nm)	λ_{em} (nm)	Toluene	Φ_f(%) THF	CH_2Cl_2	Toluene	τ(ns) THF	CH_2Cl_2
1	626	660	31.3	30.0	33.2	2.56	2.32	3.05
2	615	652	40.8	33.6	42.1	3.57	3.33	4.05
3	648	684	38.1	42.4	40.1	3.27	2.99	3.58
4	624	657	45.1	56.4	50.0	4.10	3.79	4.51
6	576	607	81.1	82.0	80.2	6.40	6.97	6.85

electron donating properties of methylpyridine or methylquinoline reduced the reactivity of the carbonyl group left at the same end. Therefore, only the mono substituted compounds can be isolated from the reaction mixture.

Fig. 2 compares the electronic absorption spectra of compound **1**–**4** with model compound N,N′-dibutyl-1,6,7,12-tetra(4-tert-butylphenoxy)perylene-3,4:9,10-tetra carboxylic diimide (**6**) [43] in dichloromethane. All of these compounds show intense absorption in the UV–vis region. The maximal absorption band of compound **1** and **2** are red-shifted for about 50 and 39 nm respectively compared with that of **6** because the introduction of quinoline or pyridine group at the carbonyl position of PDI has enlarged the conjugation system of PDI ring. The red-shift of the maximal absorption band of compound **1** is 11 nm larger than that of compound **2** because of the larger conjugation system of quinoline compared with that of pyridine. The maximal absorption bands of **3** and **4** were further red-shifted to 648 and 624 nm respectively. These significantly red-shifted maximal absorption bands relative to their precursors may be attributed to the further extension of the conjugation system because of the fixed coplanar conformation between quinoline or pyridine and PDI ring.

The fluorescence spectra of this series compounds are recorded in dichloromethane with excitation at 450 nm. Fluorescence quantum yields (Φ_f) are calculated. The spectra and experimental results are summarized in Fig. 3 and Table 1. Similar to that observed in the absorption spectra, the maximal emission band of compound **1** and **2** red-shifted significantly relative to that of model compound **6**. This can be ascribed to the extension of the conjugation system

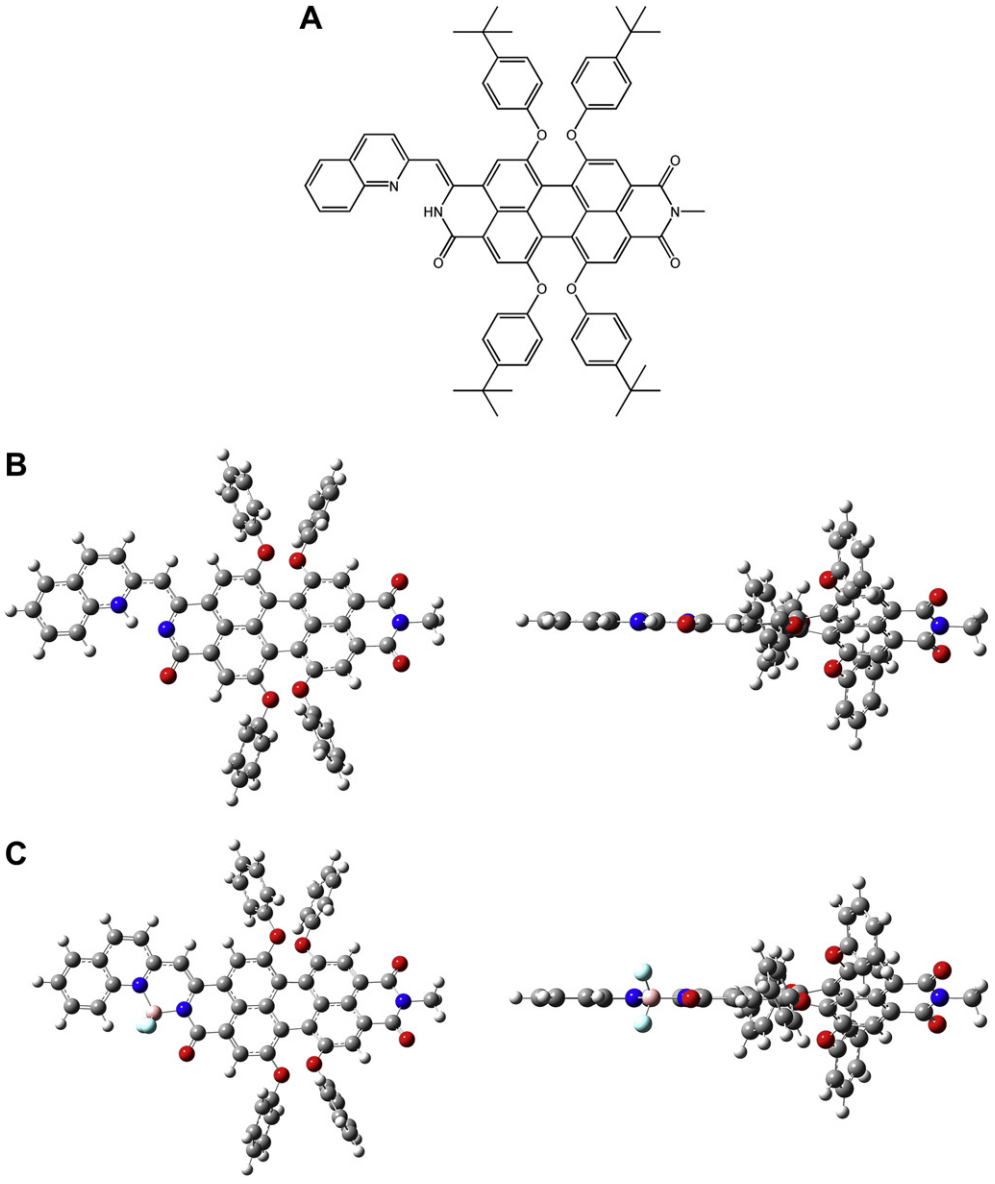

Fig. 4. The simplified molecular structure during the DFT calculation (A). The minimized structure of compound **1** (B) and **3** (C).

because of the incorporation of the quinoline or pyridine unit. The maximal emission band of compound **3** and **4** further are red-shifted to 684 and 657 nm respectively, which may be attributed to the further extension of the conjugation system because of the bonding of boron fluorid. Quinoline group in compound **3** seems more efficient on red-shifting the absorption and emission bands than the pyridine group in compound **4** as revealed by the comparison of the emission spectra of them, probably because of the larger conjugation system of the former.

Both the fluorescence quantum yields and fluorescence lifetimes of compound **1** and **2** are distinctively reduced relative to that of standard compound **6** because of the introduction of quinoline or pyridine. This might be attributed to the increased flexibility of the molecule after the introduction of side groups, which induced massive non-radiative decay for their excited states. The fluorescence quantum yields of compound **3** and **4** increased significantly relative to their precursor **1** and **2**. This can be attributed to the more rigid molecular structure of compound **3** and **4** after the bonding of boron, which reduces the non-radiative decay of the excited states.

To enhance our understanding of the relationship between molecular structures and the electronic spectra of these new PDI derivatives, we carried out structure optimization and molecular orbital (MO) calculations on compound **1**–**4** based on a simplified model with density functional theory (DFT) on the level of B3LYP. The minimized structure is shown in Fig. 4 and the calculated molecular orbital (HOMO and LUMO) energies are shown in Fig. 5. For comparison purpose, model compound **6** has also been calculated.

The minimized structure of compound **1** revealed that the quinoline group at carbonyl position presents a coplanar conformation with the PDI ring. This indicates that the quinoline group conjugated with the PDI ring efficiently through the double bond. This result is in accordance with the remarkable red-shifted absorption spectra of compound **1** relative to model **6**. Similar coplanar conformation was also observed in the minimized structure of compound **2**. The bonding of boron in compound **3** and **4** did not vary the coplanar conformation of them.

The molecular energy levels of the frontier molecular orbital shown in Fig. 5 revealed that the introduction of quinoline group at the carbonyl position has raised the energy levels of HOMO and LUMO simultaneously for compound **1** relative to that of the model compound **6**. But the increase of the HOMO is larger than that of LUMO, therefore, the energy gap between HOMO and LUMO decrease significantly. This corresponds well to the experimentally recorded red-shifted absorption spectra of compound **1**. Introduction of pyridine group has also increase the energy levels for both LUMO and HOMO, but the energy gap between HOMO and LUMO is relative larger than that in compound **1**, therefore, the absorption maximum in the absorption spectra of compound **2** is in the blue side relative to that of compound **1**.

Further bonding of boron in compound **3** and **4** do not change the planar conformation of the molecules a lot, but reduce the energy levels of HOMO and LUMO significantly. For instance, the energy level of the HOMO of compound **1** is at −4.89 eV, and it decreases to −5.12 eV in compound **3**. Similar changes are found for the energy levels of LUMOs. The energy gaps between the HOMO and LUMO of compound **3** and **4** are little bit smaller than that of compound **1** and **2** respectively, which is in accordance with the red-shifted absorption spectra of compound **3** and **4** relative to that of compound **1** and **2**.

The frontier molecular orbital maps of compound **1** as shown in Fig. 6 revealed that the contribution of the quinoline group to the HOMO and LUMO is small, but the linkage between quinoline and PDI ring contributes to the HOMO and LUMO significantly. Therefore, the red-shift on the absorption maximum for compound **1** relative to

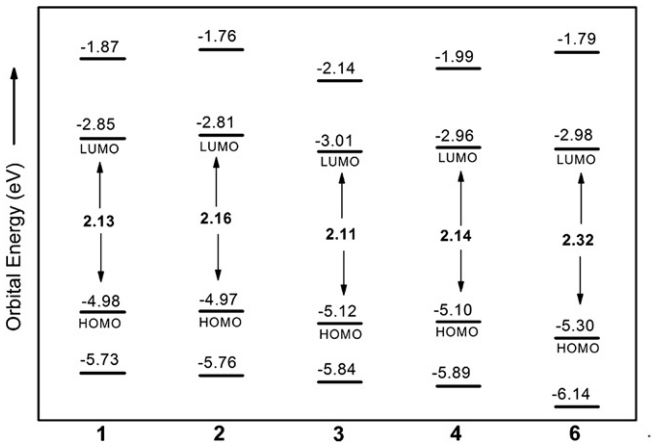

Fig. 5. Molecular orbital energy levels of compound **1**–**4** and **6**.

model **6** is dominantly caused by the double bond between the quinoline and PDI ring. In another word, the conjugation system of PDI ring does not extend to the whole quinoline ring, but is limited to the double bond between quinoline and PDI ring. Similar results can be deduced from the molecular orbital maps of compound **2** (Supporting information Fig. S1). This calculated result explains well the larger red-shift on the absorption maximum of compound **1** and **2** relative to that of model compound **6**, while the difference of the maximum absorption wavelength between compound **1** and **2** is small. The introduction of boron in compound **3** and **4** does not vary the distribution of HOMO and LUMO significantly relative to those of compound **1** and **2**. This is why the energy levels of HOMO and LUMO in compound **3** and **4** are close to that in compound **1** and **2**.

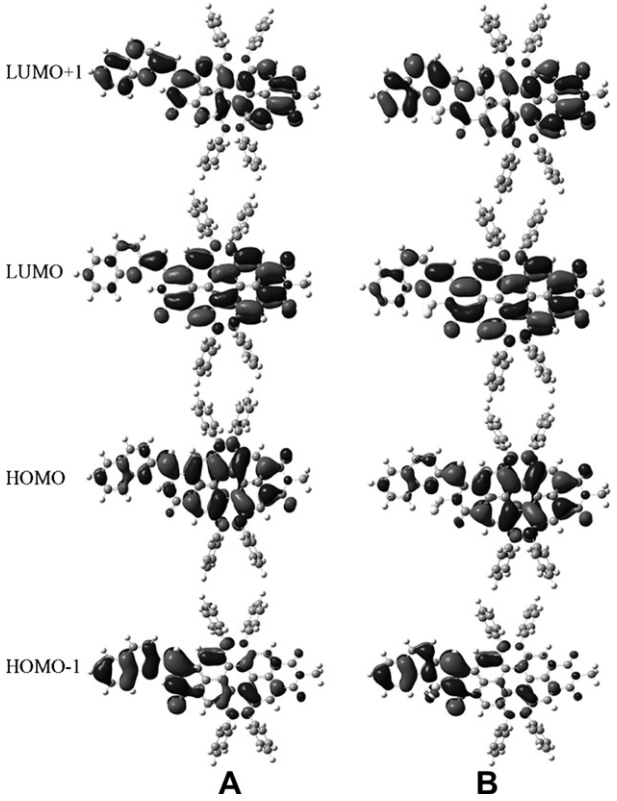

Fig. 6. Molecular orbital maps of compound **1** (A) and **3** (B).

4. Conclusions

In summary, we have successfully synthesized two novel fluorescent dyes with longer wavelength absorption and emission by introducing methylpyridine or methylquinoline groups at the carbonyl position. The new compounds can further react with $BF_3 \cdot Et_2O$ to form novel dyes with further red-shifted absorption and emission spectra. Quantum calculation suggested that the extension of the conjugation system of PDI ring is caused predominantly by the double bond between side group and the PDI ring. The nature of the side group can affect the photophysical properties of PDI, but with limited efficiency. This information is meaningful for the design of novel PDI compounds.

Acknowledgements

Financial support from the Natural Science Foundation of China (Grant No. 20771066 and 20640420467), Ministry of Education, Shandong University are acknowledged.

Appendix. Supplementary information

Supplementary information associated with this paper can be found, in the online version, at doi:10.1016/jdyepig.2010.08.014.

References

[1] Wasielewski MR. Energy, charge, and spin transport in molecules and self-assembled nanostructures inspired by photosynthesis. The Journal of Organic Chemistry 2006;71:5051–66.
[2] Elemans JAAW, Van Hameren R, Nolte RJM, Rowan AE. Molecular materials by self-assembly of porphyrins, phthalocyanines, and perylenes. Advanced Materials 2006;18:1251–66.
[3] Langhals H. Control of the interactions in multichromophores: novel concepts. Perylene bis-imides as components for larger functional units. Helvetica Chimica Acta 2005;88:1309–43.
[4] Würthner F. Perylene bisimide dyes as versatile building blocks for functional supramolecular architectures. Chemical Communications; 2004:1564–79.
[5] Jones BA, Ahrens MJ, Yoon MH, Facchetti A, Marks TJ, Wasielewski MR. High-mobility air-stable n-type semiconductors with processing versatility: dicyanoperylene-3,4:9,10-bis(dicarboximides). Angewandte Chemie International Edition 2004;43:6363–6.
[6] Yukruk F, Dogan AL, Canpinar H, Guc D, Akkaya EU. Water-soluble green perylenediimide (PDI) dyes as potential sensitizers for photodynamic therapy. Organic Letters 2005;7:2885–7.
[7] Sugiyasu K, Fujita N, Shinkai S. Visible-light-harvesting organogel composed of cholesterol-based perylene derivatives. Angewandte Chemie International Edition 2004;43:1229–33.
[8] Langhals H, Krotz O. Chiral, bichromophoric silicones: ordering principles of structural units in complex molecules. Angewandte Chemie International Edition 2006;45:4444–7.
[9] Osswald P, Leusser D, Stalke D, Würthner F. Perylene bisimide based macrocycles: effective probes for the assessment of conformational effects on optical properties. Angewandte Chemie International Edition 2005;44:250–3.
[10] Guo X, Zhang D, Zhu D. Logic control of the fluorescence of a new dyad, spiropyran–perylene diimide–spiropyran, with light, ferric ion, and proton: construction of a new three-input "AND" logic gate. Advanced Materials 2004; 16:125–30.
[11] Fan L, Xu Y, Tian H. 1,6-Disubstituted perylene bisimides: concise synthesis and characterization as near-infrared fluorescent dyes. Tetrahedron Letters 2005;46(26):4443–7.
[12] Pan J, Zhu W, Li S, Zeng W, Cao Y, Tian H. Dendron-functionalized perylene diimides with carrier-transporting ability for red luminescent materials. Polymer 2005;46:7658–69.
[13] Peneva K, Mihov G, Nolde F, Rocha S, Hotta J, Braeckmans K, et al. Water-soluble monofunctional perylene and terrylene dyes: powerful labels for single-enzyme tracking. Angewandte Chemie International Edition 2008;47:3372–5.
[14] Baumstark D, Wagenknecht H. Perylene bisimide dimers as fluorescent "Glue" for DNA and for base-mismatch detection. Angewandte Chemie International Edition 2008;47:2612–4.
[15] Langhals H, Krotz O, Polborn K, Mayer P. A novel fluorescent dye with strong, anisotropic solid-state fluorescence, small stokes' shift and high photostability – novel realizations for cooling with light. Angewandte Chemie International Edition 2005;44:2–3.
[16] Yagai S, Seki T, Karatsu T, Kitamura A, Würthner F. Transformation from H- to J-aggregated perylene bisimide dyes by complexation with cyanurates. Angewandte Chemie International Edition 2008;47:3367–71.
[17] Ji H, Majithia R, Yang X, Xu X, More K. Self-assembly of perylenediimide and naphthalenediimide nanostructures on glass substrates through deposition from the gas phase. Journal of the American Chemical Society 2008;130:10056–7.
[18] Peneva K, Mihov G, Herrmann A, Zarrabi N, Börsch M, Duncan TM, et al. Exploiting the nitrilotriacetic acid moiety for biolabeling with ultrastable perylene dyes. Journal of the American Chemical Society 2008;130:5398–9.
[19] Chen Z, Baumeister U, Tschierske C, Würthner F. Effect of core twisting on self-assembly and optical properties of perylene bisimide dyes in solution and columnar liquid crystalline phases. Chemistry – A European Journal 2007;13:450–65.
[20] Chen Z, Stepanenko V, Dehm V, Prins P, Siebbeles LDA, Seibt J, et al. Photoluminescence and conductivity of self-assembled π–π stacks of perylene bisimide dyes. Chemistry – A European Journal 2007;13:436–49.
[21] Langhals H. Cyclic carboxylic imide structures as structure elements of high stability novel developments in perylene dye chemistry. Heterocycles 1995; 40:477–500.
[22] Kazmaier PM, Hoffmann R. Theoretical study of crystallochromy. Quantum interference effects in the spectra of perylene pigments. Journal of the American Chemical Society 1994;116:9684–91.
[23] Shaller AD, Wang W, Gan H, Li ADQ. Controlled synthesis of photomagnetic nanoparticles of a Prussian blue analogue in a silica xerogel. Angewandte Chemie International Edition 2008;47:7705–9.
[24] Chao CC, Leung MK, Su YO, Chiu KY, Lin TH, Shieh SJ, et al. Photophysical and electrochemical properties of 1,7-diaryl-substituted perylene diimides. The Journal of Organic Chemistry 2005;70:4323–31.
[25] Zhao Y, Wasielewski MR. 3,4:9,10-Perylene-bis(dicarboximide) chromophores that function as both electron donors and acceptors. Tetrahedron Letters 1999;40:7047–50.
[26] Balakrishnan K, Datar A, Naddo T, Huang J, Oitker R, Yen M, et al. Effect of side-chain substituents on self-assembly of perylene diimide molecules: morphology control. Journal of the American Chemical Society 2006;128:7390–8.
[27] Zhao C, Zhang Y, Li R, Li X, Jiang J. Di(alkoxy)- and di(alkylthio)-substituted perylene-3,4;9,10-tetracarboxy diimides with tunable electrochemical and photophysical properties. The Journal of Organic Chemistry 2007;72:2402–10.
[28] Nakazono S, Imazaki Y, Yoo H, Yang J, Sasamori T, Tokitoh N, et al. Regioselective ru-catalyzed direct 2,5,8,11-alkylation of perylene bisimides. Chemistry – A European Journal 2009;15:7530–3.
[29] Qian H, Wang Z, Yue W, Zhu D. Tetrachloroperylene bisimide: combination of Ullmann reaction and C–H transformation. Journal of the American Chemical Society 2007;129:10664–5.
[30] Avlasevich Y, Müller S, Erk P, Müllen K. Novel core-expanded rylenebis (Dicarboximide) dyes bearing pentacene units: facile synthesis and photophysical properties. Chemistry – A European Journal 2007;13:6555–61.
[31] Pschirer NG, Kohl C, Nolde F, Qu J, Müllen K. Pentarylene- and hexarylenebis (dicarboximide)s: near-infrared-absorbing polyaromatic dyes. Angewandte Chemie International Edition 2006;45:1401–4.
[32] Zhen Y, Qian H, Xiang J, Qu J, Wang Z. Highly regiospecific synthetic approach to monobay-fuctionalized perylene bisimide and Di(perylene bisimide). Organic Letters 2009;11:3084–7.
[33] Qian H, Yue W, Zhen Y, Motta S, Donato E, Negri F, et al. Heterocyclic annelated di(perylene bisimide): constructing bowl-shaped perylene bisimides by the combination of steric congestion and ring strain. The Journal of Organic Chemistry 2009;74:6275–82.
[34] Langhals H, Jaschke H, Ring U, von Unold P. Imidazolo perylene imides: a highly fluorescent and stable replacement of terrylene. Angewandte Chemie International Edition 1999;38:201–3.
[35] Quante H, Geerts Y, Müllen K. Synthesis of soluble perylenebisamidine derivatives. Chemistry of Materials 1997;9:495–500.
[36] Oliveira LS, Corrêa DS, Miaoguti L, Constantino CJL, Aroca RF, Zilio C, et al. Perylene derivatives with large two-photon-absorption cross-sections for application in optical limiting and upconversion lasing. Advanced Materials 2005;17:1890–3.
[37] Langhals H, Kirner S. Novel fluorescent dyes by the extension of the core of perylenetetracarboxylic bisimides. European Journal of Organic Chemistry 2000;2:365–80.
[38] Li Y, Li Y, Li J, Li C, Liu X, Yuan M, et al. Synthesis, characterization, and self-assembly of nitrogen-containing heterocoronene-tetracarboxylic acid diimide analogues: photocyclization of N-heterocycle-substituted perylene bisimides. Chemistry – A European Journal 2006;12:8378–85.
[39] Feng J, Liang B, Wang D, Xue L, Li X. Novel fluorescent dyes with fused perylene tetracarboxlic diimide and BODIPY analogue structures. Organic Letters 2008;10:4437–40.
[40] Becke AD. Density-functional exchange-energy approximation with correct asymptotic behavior. Physical Review A 1998;38:3098–100.
[41] Becke AD. Density-functional thermochemistry. III. The role of exact exchange. Journal of Chemical Physics 1993;98:5648–52.
[42] Ong KK, Jensen JO, Hameka HF. Theoretical studies of the infrared and Raman spectra of perylene. Journal of Molecular Structure: THEOCHEM 1999;459:131–44.
[43] Feng J, Zhang Y, Zhao C, Li R, Xu W, Li X, et al. Cyclophanes of perylene tetracarboxylic diimide with different substituents at bay positions. Chemistry – A European Journal 2008;14:7000–10.
[44] Zhou Y, Xiao Y, Chi S, Qian X. Isomeric boron–fluorine complexes with donor–acceptor architecture: strong solid/liquid fluorescence and large stokes shift. Organic Letters 2008;10:633–6.
[45] Zhou Y, Xiao Y, Li D, Fu M, Qian X. Novel fluorescent fluorine–boron complexes: synthesis, crystal structure, photoluminescence, and electrochemistry properties. The Journal of Organic Chemistry 2008;73:1571–4.